BIOCHEMISTRY
including biophysical chemistry & molecular biology

Article

pubs.acs.org/biochemistry

Probing the RNA Binding Surface of the HIV-1 Nucleocapsid Protein by Site-Directed Mutagenesis

Wei Ouyang,[†,§] Stephen Okaine,[‡,∥] Mark P. McPike,[‡,⊥] Yong Lin,[‡,@] and Philip N. Borer*[,†,‡]

[†]Graduate Program in Structural Biology, Biochemistry, and Biophysics and [‡]Department of Chemistry, Syracuse University, Syracuse, New York 13244-4100, United States

Supporting Information

ABSTRACT: The highly conserved nucleocapsid protein domain in HIV-1 recognizes and binds SL3 in genomic RNA. In this work, we used the structure of the NCp7−SL3 RNA complex to guide the construction of 16 NCp7 mutants to probe the RNA binding surface of the protein [De Guzman, R. N., et al. (1998) *Science 279*, 384−388]. Thirteen residues with functional or structural significance were mutated individually to Ala (Asn[5], Phe[6], Val[13], Phe[16], Asn[17], Gly[19], Glu[21], Ile[24], Gln[45], Met[46], Gly[22], Pro[31], and Gly[40]), and three salt bridge switch mutants exchanged Lys and Glu (Lys[14]−Glu[21], Lys[33]−Glu[42], and Lys[38]−Glu[51]). Dissociation constants (K_d) determined by fluorescence titration and isothermal titration calorimetry were used to compare affinities of SL3 for the variant proteins to that for the wild type. The F16A (Phe[16] to Ala) variant showed a 25-fold reduction in affinity, consistent with a loss of organized structure in f1, the protein's first zinc finger. I24A, Q45A, and M46A reduced affinity by 2−5-fold; these residues occupy nearly equivalent positions in f1 and f2. E21A increased affinity by 3-fold, perhaps because of the mutant's increased net positive charge. Among the salt bridge switch mutants, only K14E/E21K in f1 caused a substantial change in affinity (5-fold reduction), binding SL3 with a biphasic binding isotherm. Aside from these six variants, most of the mutations studied have relatively minor effects on the stability of the complex. We conclude that many side chain interactions in the wild-type complex contribute little to stability or can be compensated by new contacts in the mutants.

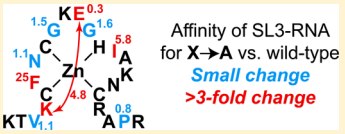

NCp7 is the mature nucleocapsid protein of HIV-1. This highly conserved 7 kDa protein consists of 55 amino acid residues and contains two CCHC-type zinc knuckle structures (Cys-X2-Cys-X4-His-X4-Cys, where X is a variable amino acid),[1] as shown in Figure 1. NC domains of Gag-precursor polyproteins bind specifically to full-length genomic RNA and recruit gRNA molecules to newly forming virions. In immature HIV-1 virions, there are 2000−3000 Gag precursors coating the dimeric viral RNA, equivalent to approximately one NC protein per seven nucleotides.[2−4] This histonelike coat protects viral RNA or proviral DNA from nuclease digestion.[5,6] As the virus matures, the Gag polyprotein is proteolyzed by the viral protease into several structural proteins, including NCp7.[7,8] The NC protein is multifunctional in retroviruses and acts in almost every stage of the virus replication cycle.[9−11] In the early phase of the replication cycle, mature NC proteins interact with the viral RNA genome, primer tRNA, and other viral proteins, e.g., reverse transcriptase and the accessory protein Vpr,[12−16] to assist in proviral DNA synthesis and stable integration into the host genome.[17] In the late phase, the NC domain in the Gag precursor protein recognizes viral genomic RNA, facilitates its dimerization,[18−20] and ensures correct packaging of the virion.[7,21−25] NCp7 is frequently used as a model for the NC domain.[26]

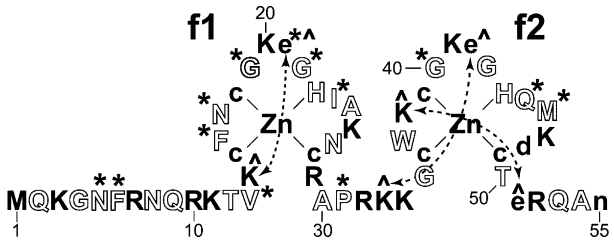

Figure 1. HIV-1 NCp7 protein. Residues carrying a charge at neutral pH are shown with filled letters (uppercase for positive and lowercase for negative); Zn_2·NCp7(1−55) carries a charge of +9 at neutral pH.[43] The sequence for the pNL4-3 isolate is shown. Residues that were mutated to alanine in this study are denoted with asterisks; residues in salt bridge switches are denoted with carets, with bridges denoted by dashed arrows. (The reader may also see Figure S4 of the Supporting Information and Figure 3 for a comprehensive view of the rationale for choosing the particular mutants to be tested.)

The NC domain specifically recognizes and binds tightly to a RNA motif in the 5′-leader of the HIV-1 viral genome, named stem−loop 3 or SL3, as shown in Figure 2. SL3 is the primary recognition site for the NC domain and is highly conserved in sequences among different strains of HIV-1, which makes it of particular interest to many researchers.[1,10,27−33] The NC protein interacts with RNA via its conserved CCHC zinc finger motifs.[34−36] The zinc fingers, especially the intact N-terminal zinc finger (f1), are required for the binding specificity and target selectivity of the NC domain for viral genomic RNA.[37,38] Mutations in the zinc fingers that render them incompetent for zinc binding can destroy the NC protein's

Received: January 31, 2013
Revised: April 12, 2013
Published: April 17, 2013

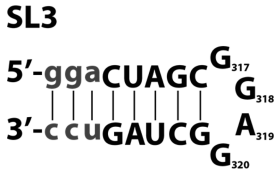

Figure 2. SL3 RNA. A 20-mer synthetic RNA molecule used in this study as a model for SL3. The core sequence is shown in bold uppercase letters. The numbering of the nucleotides is the same as in the HIV-1 RNA genome.

capacity to recognize and package viral genomic RNA[39−41] and have a negative impact on virion biogenesis and maturation.[42] At physiological ionic strengths, NCp7 favors a 1:1 complex with SL3 RNA,[1,43,44] but other ratios have also been observed, especially at lower salt concentrations.[45,46] Electron paramagnetic resonance (EPR) studies show that the intact zinc fingers can help maintain the overall structure of NCp7 in the complex[44] and are required to immobilize SL3 RNA in $R_1P_{n>1}$ complexes in a low-ionic strength solution.[45] NMR and mutational studies show that the short conserved linker between the two zinc fingers, ^{29}RAPRKKG^{35}, is critical for virion structure and infectivity.[47,48] The basic residues in the NC domain have nonspecific interactions with RNA and can promote virion assembly without the zinc fingers and viral genomic RNA.[49] Mutation of the basic residues in the NC protein reduces its affinity for RNA proportionally.[50,51] Molecular dynamics studies confirm that the primary interactions between NCp7 and viral genome are electrostatic interactions between NCp7's basic residues and the nucleic acid. The complex is further stabilized by nonelectrostatic interactions such as hydrophobic stacking.[24]

Drugs that target the nucleocapsid have the potential to interfere with critical functions at many stages of the viral life cycle.[52,53] Many small molecule drug candidates aimed at the nucleocapsid protein have been developed and investigated as potential HIV treatments.[54−61] Investigation of the details of interactions between NCp7 and SL3 could shed light on designing anti-HIV drugs.

In the NMR structure of the NCp7−SL3 complex,[1] some residues are of special interest because of their direct side chain interactions with RNA or other residues in the protein. A survey of 1700 NCp7 sequences is summarized in Figure 3, showing the conservation of each residue and their side chain interactions based on the NMR structure of the complex.[1,62] An important residue is Trp^{37}, which stacks on G^{318} of SL3 RNA,

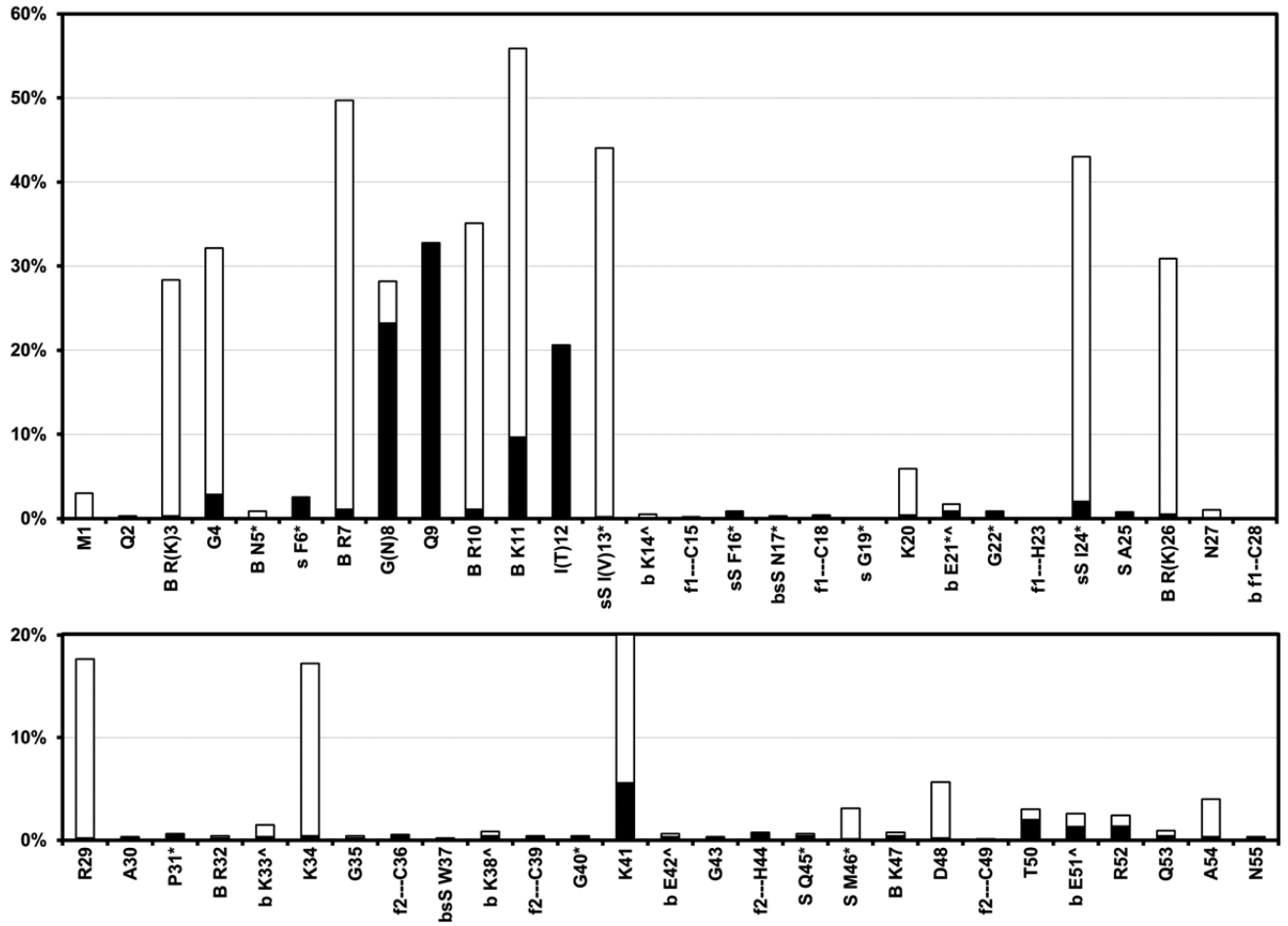

Figure 3. Variation in 1700 NCp7 sequences: *X*-axis, residue position and name; *Y*-axis, percentage of variation in each residue position; white bars, conservative amino acid substitutions; black bars, nonconservative amino acid substitutions. Notation for RNA−protein side chain interactions in the SL3−NCp7 complex: B for H-bonds or salt bridges and S for steric contacts. Side chain protein−protein contacts are noted as follows: b for H-bonds or salt bridges and s for steric contacts.[1] The consensus sequence is shown, with different residues in the pNL4-3 isolate used in this work noted in parentheses.[62] CCHC fragments in fingers, f1 and f2, are marked. Residues that were mutated to alanine in this study are denoted with asterisks; residues in salt bridge switches are denoted with carets.

dx.doi.org/10.1021/bi400125z | *Biochemistry* 2013, 52, 3358−3368

leading to nearly full quenching of its fluorescence and allowing the straightforward analysis of binding isotherms used in this study.[1,26,35,63−65] NCp7 has a hydrophobic core consisting of Val[13], Phe[16], Ile[24], Ala[25], Trp[37], Gln[45], and Met[46],[24,35,66] which extensively interacts with SL3 RNA. Among them, Phe[16] and Trp[37] are perhaps the most important because of their interactions with the bases in the SL3 RNA loop.[1] Asn[5] in the N-terminal 3_{10} helix is the only NCp7 residue forming hydrogen bonds with the SL3 RNA stem. There are also salt bridges between Lys[14] and Glu[21] and between Lys[38] and Glu[51], which appear to stabilize the zinc fingers, and between Lys[33] and Glu[42], which helps to stabilize the folding of f2 against the short linker between the fingers. By substituting alanine for the residues that have direct side chain interactions with SL3 RNA or other protein residues, we can probe the key interactions between NCp7 and SL3 RNA. Our results complement our previous work that focused on the contribution of individual SL3 bases to the interaction with NCp7.[63]

EXPERIMENTAL PROCEDURES

Site-Directed Mutagenesis. The pRD2 construct of the NCp7 subclone (HIV-1 strain pNL4-3) was used as a wild-type NCp7 template[67] (a generous gift from M. Summers of the University of Maryland, Baltimore County, Baltimore, MD). Site-directed mutagenesis was conducted using the Stratagene (now Agilent Genomics) QuikChange or QuikChange II site-directed mutagenesis kit. Primers were designed using the Stratagene QuikChange Primer Design Program (http://www.genomics.agilent.com) or PrimerX online tool (http://bioinformatics.org/primerx/) and synthesized by Integrated DNA Technologies, Inc. (Coralville, IA). The mutagenesis polymerase chain reactions were set up according to the manufacturer's instructions. Mutants were made using primers listed in Table S1 of the Supporting Information. Double mutants were made through two consecutive site mutagenesis experiments, mutating one residue at a time and using the product from the first mutagenesis as the intermediate template for the second mutagenesis. The mutated plasmids were transformed into *Escherichia coli* XL1-Blue cells (Agilent) for plasmid preservation and propagation. Plasmids prepared from the XL1-Blue strains were then subjected to Sanger sequencing, and the confirmed plasmids with desired mutations were transformed into *E. coli* BL21-(DE3)pLysS cells (Agilent) for recombinant protein overexpression.

NCp7 Protein Preparation. The cells were grown and harvested, and the proteins were purified using a revised protocol based on that of Lee et al.[67] and Shubsda et al.[26] A single colony was used to inoculate a 5 mL starter culture in LB medium containing 1× M9 salts,[68] 0.4% glucose, 100 μM $ZnCl_2$, 100 μg/mL ampicillin, and 34 μg/mL chloramphenicol. The starter culture was grown at 37 °C overnight and added to 1 L of LB medium containing the same supplements as described above. The cells were grown at 37 °C to an absorbance of 0.6−0.8 at 600 nm before being induced with 400 μM IPTG [isopropyl β-D-thiogalactopyranoside (Sigma-Aldrich)]. The induced cells were grown for an additional 4 h and harvested by centrifugation at 5000 rpm for 15 min (Beckman Coulter Avanti J-E centrifuge, JLA-10.5 rotor). Cell pellets from a 1 L culture were resuspended on ice in 30 mL of lysis buffer {50 mM Tris-HCl (pH 8.0), 10% (v/v) glycerol, 0.1 M NaCl, 1 μM $ZnCl_2$, 5 mM TCEP·HCl [tris(2-carboxyethyl)-phosphine hydrochloride (Thermo Pierce)], 60 μg/mL lysozyme, 53 μM PMSF [phenylmethanesulfonyl fluoride (Sigma-Aldrich)], 1 μg/mL Pepstatin A (Sigma-Aldrich)}; 2.1 mL of 1% (w/v) sodium deoxycholate was added to the resuspended cells. The mixture was left on ice for 20 min before 4 mL of B-PER II reagent (Thermo Pierce) was added. The cells were then left on ice for 10 min before being subjected to sonication for 4 × 25 s at an output power of 20−25 W. Two milliliters of 4% PEI [polyethyleneimine (Sigma-Aldrich)] was then added to the mixture to precipitate nucleic acids. The lysed cells were centrifuged at 17000 rpm for 30 min at 4 °C (Beckman Coulter Avanti J-E centrifuge, JA-25.5 rotor), and the supernatant was collected for FPLC purification. Cell lysates were loaded onto a HiPrep Q FF and a HiPrep SP FF column (GE Healthcare) connected in series and previously equilibrated with 200 mL of buffer A [50 mM Tris-HCl (pH 8.0), 10% (v/v) glycerol, 0.1 M NaCl, 1 μM $ZnCl_2$, and 1 mM TCEP·HCl]. The NCp7 protein was eluted using a 1 h linear gradient from 20 to 50% buffer B [50 mM Tris-HCl (pH 8.0), 10% (v/v) glycerol, 1 M NaCl, 1 μM $ZnCl_2$, and 1 mM TCEP·HCl]. The homogeneity of the eluted protein was determined by SDS−PAGE. The purified NCp7 protein fractions were then pooled and concentrated using a VIVASPIN 15 mL concentrator (5000 molecular weight cutoff) (GE Healthcare). The NCp7 concentration was determined by UV absorption as described previously.[26] The sample purity and homogeneity were further confirmed by MALDI-TOF mass spectrometry and analytical ultracentrifugation. Purified NCp7 wild-type and mutant proteins were stored at −80 °C in aliquots.

Mass Spectrometry. Purified and concentrated protein samples were dialyzed overnight against MS buffer [5 mM sodium phosphate, 0.2 M NaCl, 1 μM $ZnCl_2$, and 1 mM TCEP·HCl (pH 7.0)]. The concentrations of the dialyzed samples were determined by UV using MS buffer as a blank. The samples were then diluted to 20 μM in a 0.1% aqueous trifluoroacetic acid (TFA) solution. The dilute samples were then mixed in a 1:1 ratio with a freshly prepared matrix solution (saturated sinapinic acid in a 1:2 acetonitrile/0.1% aqueous TFA mixture); 1 μL of each sample mixture was spotted onto a MALDI sample plate and dried in air. The mass spectra were measured in reflectron mode on a Bruker Daltonics Autoflex III Smartbeam MALDI-TOF system. The observed molecular weight and the calculated molecular weight of purified NCp7 wild-type and mutant proteins are listed in Table S2 of the Supporting Information.

Analytical Ultracentrifugation. Protein samples were dialyzed overnight against MS buffer. The concentrations of the dialyzed samples were determined by UV using MS buffer as a blank. Samples were then diluted in MS buffer to an absorbance of 1−1.5 at 280 nm before being loaded onto a Beckman Coulter ProteomeLab XL-A Protein Characterization System; 400 μL of the sample was loaded each time. Sedimentation velocity experiments were conducted at 50000 rpm and 10 °C. Sedimentation data were collected at 280 nm and analyzed using SEDFIT.[69]

SL3 RNA. Desalted SL3 RNA (rGrGrArCrUrArGrCrGrG-rArGrGrCrUrArGrUrCrC) was purchased from IDT and reconstituted in NCp7 titration buffer [5 mM sodium phosphate, 0.2 M NaCl, 1 μM $ZnCl_2$, 1 mM TCEP·HCl, and 0.1% PEG 8000 (pH 7.0)]. The purity of SL3 RNA was examined by high-performance liquid chromatography and confirmed to be higher than 90%.[70] The concentration of SL3 RNA was determined by UV as described previously.[26]

NCp7–SL3 Trp Titration Assay. NCp7 wild-type and mutant proteins were titrated with SL3 RNA using assay conditions similar to those described previously[26] in NCp7 titration buffer. Wild-type NCp7 protein was titrated every time as a positive control along with the mutant proteins. The fluorescence was measured at 350 nm with a PTI Quanta-Master QM-4/2003SE fluorometer using a 290 nm excitation wavelength, a 4 nm excitation band-pass, and a 1.5 nm emission band-pass. The fluorescence titration curves were fit to a model assuming a 1:1 stoichiometry for the ratio of NCp7 to bound SL3 RNA as described by Paoletti et al.[63] The titration curves were fit to the following equation:

$$(I - I_\infty)/I_0 = \{-(R_t - P_t + K_d) + [(R_t - P_t + K_d)^2 + 4P_tK_d]^{1/2}\}/(2P_t) \quad (1)$$

where R_t and P_t are the total RNA and protein concentrations, respectively, I_0 is the intensity at $R_t = 0$, and I_∞ is the limiting intensity at saturation. In this work we set I_∞ equal to 0. The titration data were fit, and K_d values were obtained using Origin version 7.0 (OriginLab, Northampton, MA) as described previously.[43] The NCp7 concentration was fixed at 0.3 μM, and titrations were extended to an R_t/P_t value of at least 3.

Isothermal Titration Calorimetry. Isothermal titration calorimetry (ITC) experiments were performed using a Microcal VP-ITC MicroCalorimeter (Microcal, now GE Healthcare). Origin version 7.0 (OriginLab) was used for data collection and analysis. First, 1.4 mL of 5 μM SL3 RNA dissolved in NCp7 titration buffer was added to the calorimetric cell; 300 μL of 45 μM NCp7 protein was used as the titrant in each titration. Reactions were conducted at 30 °C. The reference power was set to 20 μcal/s. The first injection was set to 2 μL over 4 s, followed by 29 injections of 10 μL over 20 s. The last injection was set to 8 μL over 16 s. The interval between each injection was set to 240 s. The syringe stirring speed was set to 295 rpm. The feedback gain was set to high, and the equilibrium was set to fast, auto. Binding isotherms were fit to a one-binding site model using the supplied ITC add-on for Origin version 7.0 from the manufacturer (Microcal, now GE Healthcare). A baseline was drawn by linear extrapolation using the data points collected under saturation conditions and subtracted from the whole data set to correct for the heat of dilution.[71]

RESULTS

Sixteen mutant proteins were prepared as laid out in Figure S1 and Table S1 of the Supporting Information, including 13 single mutants and three double mutants. All but three mutants target residues that had been predicted to be involved in side chain contact with SL3 or in salt bridges.[1] The targeted residues in the other three mutants, even though they are not predicted to be involved in any side chain contacts, are highly conserved and either structurally rigid (Pro^{31}) or flexible (Gly^{22} and Gly^{40}) (see Figure 3 and Figure S1 of the Supporting Information). The 13 single mutants were made by substituting alanine for one non-alanine residue in the wild-type NCp7 sequence. The other three mutants were introduced with double mutations, resulting in position switching of two residues in the wild-type (WT) coding sequence. The switched residues were predicted to form salt bridges with each other based on their spatial proximity and opposite charges in their side chains. With a switch of the position of the two residues, the salt bridge could still form between them if the rest of the protein structure remained undisturbed. If the main function of those residue pairs in NCp7's interaction with SL3 RNA can be attributed to the salt bridges, then the affinity of the resulting double mutants for SL3 should not be significantly affected.

Mutant proteins were purified and stored at −80 °C for long periods of time. Gel analysis and affinity assays suggested that the proteins can stay viable for months without significant degradation under the storage conditions. SDS–PAGE gels confirmed that the purified proteins were at least 95% pure.[70] Molecular weights of all mutant proteins were measured by MALDI-TOF mass spectrometry and compared to the calculated molecular weights. The results are listed in Table S2 of the Supporting Information.

To further confirm the protein purity and the aggregation status of NCp7 under assay conditions, we examined the protein samples by AUC. The results indicated that the protein samples do not aggregate to form dimers or oligomers under conditions used in the affinity assays.[70]

Figure 4 shows several titration curves from the tryptophan fluorescence titration assay. For a clearer view, only four of the

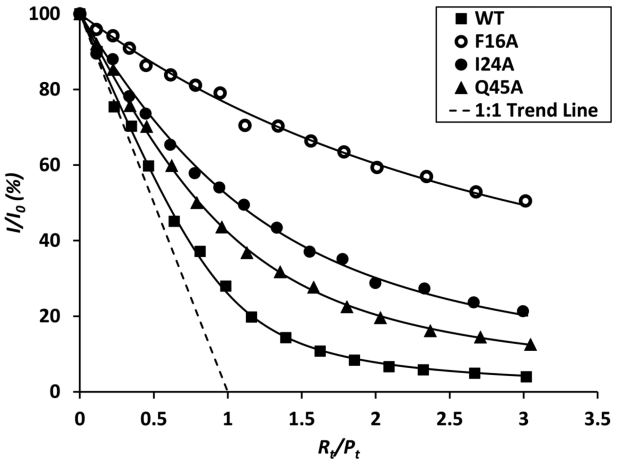

Figure 4. Fluorescence titration of NCp7 wild-type and mutant proteins with SL3 RNA. The total RNA:total protein ratio, R_t/P_t, increases from left to right. Optimized fits (—) for 1:1 complexes have K_d values listed in Table 1 (see Experimental Procedures and Results for details of the fitting). Data points are as follows: (■) NCp7 wild type, (○) F16A, (●) I24A, and (▲) Q45A. The dashed line is the trend line for a 1:1 complex with an infinite binding constant (K_d^{-1}).

17 protein–SL3 titration curves are shown, representing a wide range of the K_d values for the binding of SL3 to the WT and mutant NCp7 proteins (Figure S2 of the Supporting Information shows three more titration curves; all curves are included in ref 70). All 17 K_d values calculated from the Trp titration assay are reported in Table 1, ranging from 8.6 to 720 nM. The K_d value for the WT–SL3 complex was calculated to be 29 nM, which agreed with our previous experimental data[43,63] and served as a good positive control for the mutant proteins. Dissociation constants were optimized to obtain the best fit titration curves, assuming a 1:1 complex. No evidence of other stoichiometries was indicated by the data at 0.2 M NaCl.[26,43] The binding isotherms for low-affinity complexes were not extended to saturation because the nature of the complex may change in the presence of a large excess of RNA.[63] We assumed an I_∞ of 0 because in the range of the K_d values for these titration curves, very little residual fluorescence was observed.[43,63]

dx.doi.org/10.1021/bi400125z | Biochemistry 2013, 52, 3358–3368

Table 1. Tryptophan Fluorescence Titration Results for NC Proteins Binding SL3 RNA

	K_{dTrp} (nM)				
	avg	SD	F^a	SD	m^b
WT	29	±4.5	1.0	±0.15	8
N5A	29	±5.6	1.0	±0.19	5
F6A	33	±3.3	1.1	±0.11	3
V13A	31	±6.9	1.1	±0.24	3
F16A	720	±26	25	±0.90	3
N17A	32	±1.4	1.1	±0.05	3
G19A	45	±2.6	1.5	±0.09	3
E21A	8.6	±2.3	0.3	±0.08	3
G22A	45	±6.7	1.6	±0.23	3
I24A	170	±29	5.8	±0.99	5
P31A	23	±5.8	0.8	±0.20	3
G40A	33	±6.5	1.1	±0.22	3
Q45A	73	±14	2.5	±0.49	4
M46A	62	±10	2.1	±0.35	3
K14E/E21K	140	±5.1	4.8	±0.17	7
K33E/E42K	40	±11	1.4	±0.37	3
K38E/E51K	33	±5.1	1.1	±0.18	3

[a] F is the factor by which the K_d of a mutant NC protein changes from that of NCp7. F = (K_d of mutant)/(K_d of WT). F values for each K_d measurement over the average K_d of WT were determined, and then the averages of the F values were taken and standard deviations of F values calculated from the replicates and recorded. [b] Number of measurements.

Wild-type NCp7 and eight mutant NC proteins were also examined using ITC assays. The K_d values calculated from the ITC assays (termed K_{dITC}) were compared with those calculated from the tryptophan fluorescence titration assays (termed K_{dTrp}). Taking into account the fact that ITC experiments were conducted at 30 °C, we converted the K_d values calculated from the ITC data to 22 °C using the van't Hoff equation as shown in eq 2, assuming that $\Delta H°$ is constant over this small temperature range. The average number of binding sites determined by ITC also suggested that NC–SL3 binding follows a 1:1 binding model. The results are compiled in Table 2. Sample ITC titration curves are shown in Figure 5 and Figure S3 of the Supporting Information.

$$\ln\left(\frac{K_{d1}}{K_{d2}}\right) = \frac{\Delta H°}{R}\left(\frac{1}{T_1} - \frac{1}{T_2}\right) \quad (2)$$

DISCUSSION

Figure 6 summarizes the change in the affinity of mutant proteins for SL3 RNA compared to that of the WT. For the sake of convenience, the mutants are grouped according to the change in K_d calculated from the tryptophan titration assay. The factor, F, by which K_d changes is listed in Table 1 for each protein. Mutants with F values of <2 are considered as mutants of little or no change in affinity. The mutants with F values between 2 and 10 or between 0.1 and 0.5 are considered to have a moderate change in affinity. Those with F values of >10 are considered as mutants exhibiting a significant change in affinity. The K_d changes are also charted in Figure S4 of the Supporting Information.

Single Mutants Exhibiting Little or No Change in Affinity for NCp7. Most of the tested mutants have a K_d value close to that of the WT. These mutants include N5A, F6A, V13A, N17A, G19A, G22A, P31A, G40A, and two of the double mutants, K33E/E42K and K38E/E51K.

Phe[6] does not participate in any RNA–protein side chain contacts, but the phenyl side chain packs with Val[13] and Ile[24].[1] This does not appear to contribute much to the stabilization of the structure of the protein in a complex with the RNA.

Considering the high degree of conservation and the position and structure of Gly[19], Gly[22], and Gly[40] (each reside in one of the two zinc finger motifs), we hypothesized that substitution of alanine might cause unwanted methyl group contacts between the NC protein and RNA, or within the protein itself, protein or reduced flexibility in the zinc fingers. The observation, however, indicated the opposite, that substitutions of alanine for glycine on these positions do not cause unfavorable effects on the affinity of NCp7 for SL3.

Pro[31] itself does not have any RNA–protein or protein–protein side chain contact, but given its unique structural rigidity and high degree of conservation, we expected that the P31A mutation might affect its affinity for SL3 RNA. It has been reported that Pro[31] helps determine the spatial proximity of the two zinc fingers,[47] which would be important for viral RNA dimerization, virion formation, and infectivity.[47,48] Thus, the observation that the P31A mutant shows only a slight change in affinity for SL3 RNA was surprising. It appears that

Table 2. ITC Titration Results for NC Proteins Binding SL3 RNA

	K_{dITC} (nM)				N^c		$\Delta H°$ (kcal/mol)		
	30 °C	RT[a]	SD	F^b	avg	SD	avg	SD	m^d
WT	69	42	±5.0	1.0	1.1	±0.034	-11×10^3	±600	4
N5A	124	80	±26	1.9 (1.0)	1.1	±0.082	-9.8×10^3	±1500	4
F6A	97	58	±23	1.4 (1.1)	0.87	±0.041	-12×10^3	±690	3
F16A	1790	1200	±540	28 (25)	1.4	±0.13	-9.0×10^3	±2500	3
I24A	483	310	±130	7.3 (5.8)	1.4	±0.18	-9.0×10^3	±910	4
P31A	81	46	±5.6	1.1 (0.8)	1.1	±0.044	-13×10^3	±320	3
Q45A	177	120	±12	2.8 (2.5)	1.2	±0.087	-8.2×10^3	±360	3
K14E/E21K	195	150	±14	3.5 (4.8)	0.79	±0.021	-6.3×10^3	±430	3
K33E/E42K	75	43	±4.1	1.0 (1.4)	1.1	±0.049	-12×10^3	±1100	3

[a] K_d values measured at 30 °C were converted to equivalents at room temperature (RT, 22 °C) using the van't Hoff equation. The K_d values at 22 °C are rounded to two significant digits. [b] F is the factor by which the K_d of a mutant NC protein changes from that of NCp7. F = (K_d of mutant)/(K_d of WT). The numbers in parentheses show the F factors from the Trp titrations for easy comparison. [c] Average number of binding sites determined by ITC. [d] Number of measurements.

dx.doi.org/10.1021/bi400125z | Biochemistry 2013, 52, 3358–3368

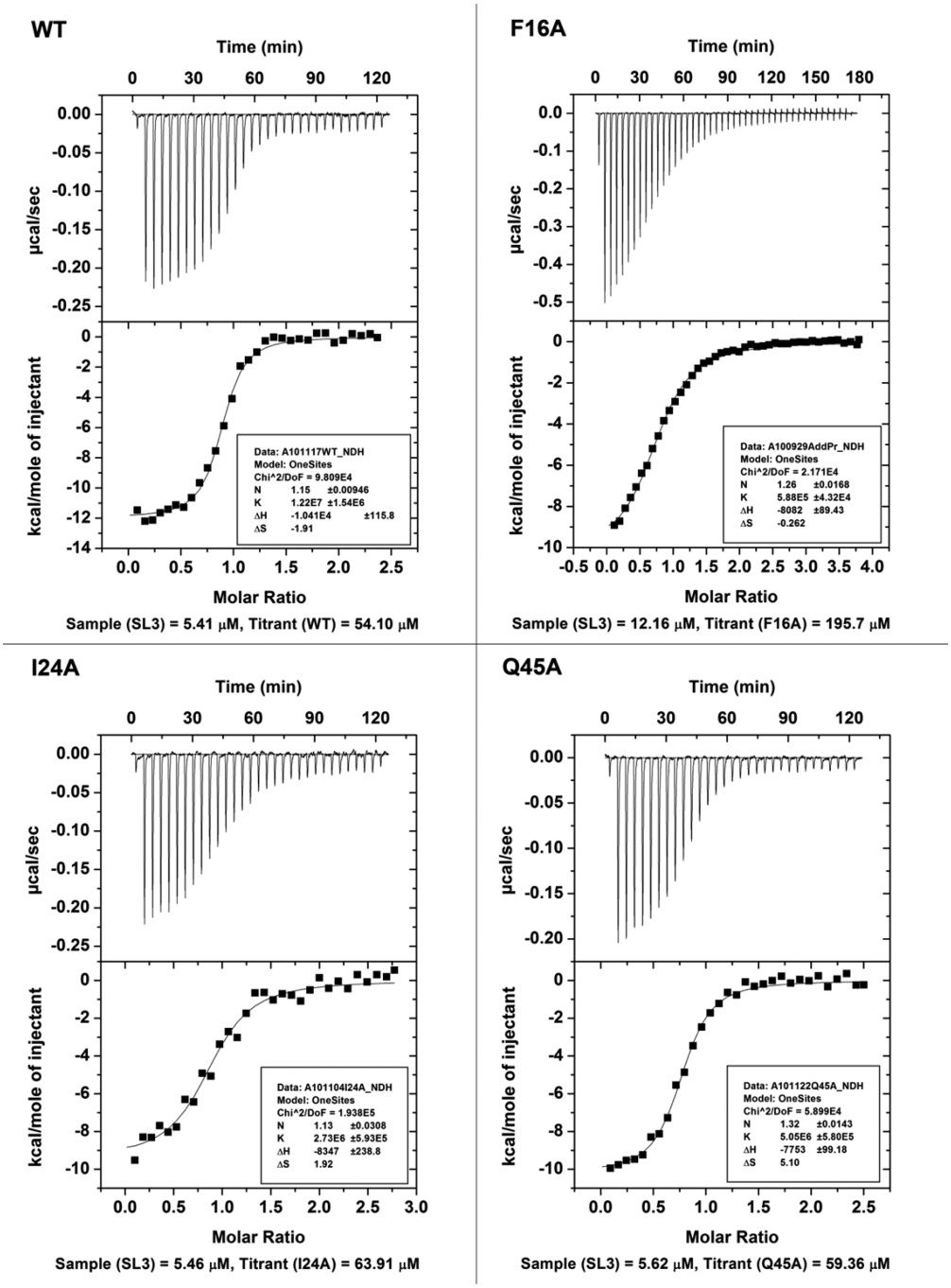

Figure 5. ITC curves of NCp7 WT and mutant proteins with SL3 RNA. Protein names are given at the top left of each panel. K_d values and other binding parameters are listed in Table 2. Note that the *Y*-axes of the panels are not all on the same scale.

the affinity of NCp7 for SL3 RNA does not require Pro^{31} to orient the zinc fingers.

Val^{13} participates in the NCp7−SL3 interaction by forming a hydrophobic cleft, which interacts with G^{320} of SL3 RNA along with f1 residues Phe^{16}, Ile^{24}, and Ala^{25}. In the complex, Val^{13} also contributes to intraprotein hydrophobic interactions between the 3_{10} helix and zinc finger 1.[1] Molecular dynamics studies suggest that Val^{13} resides within a hydrophobic core along with Phe^{16}, Ile^{24}, Ala^{25}, Trp^{37}, Gln^{45}, and Met^{46}.[35,66] Substitution of Val^{13} with alanine shortens the side chain but maintains a hydrophobicity similar to that of valine. The observation that the V13A mutation resulted in a change in affinity smaller than those seen for the other mutants in the hydrophobic core suggests that Val^{13} contributes little to the RNA binding function of NCp7, except by maintaining the hydrophobic core. The fact that Val^{13} is among the residues with a higher frequency of natural variations with hydrophobic residues[62] also suggests that the specific side chain of Val^{13} is less important to maintaining the hydrophobic core than some of the other residues.

Asn^5 and Asn^{17} were thought to play a significant role in the recognition of SL3 by NCp7.[1] Asn^5 is part of the 3_{10} helix that binds the major groove of SL3 RNA and is also the only NCp7 residue that forms specific hydrogen bonds with the RNA stem (side chain carbonyl to C322 N4H group). Moreover, Asn^5 is one of the most conserved residues in NC. Asn^{17} is part of the

dx.doi.org/10.1021/bi400125z | *Biochemistry* 2013, 52, 3358−3368

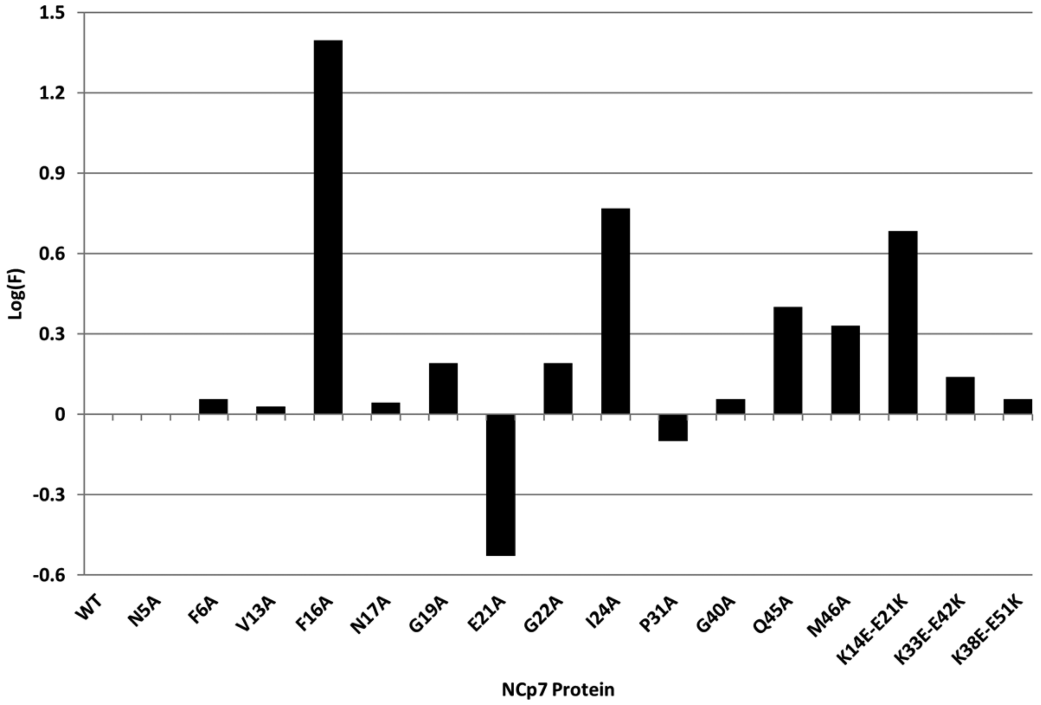

Figure 6. Effect of site-directed mutagenesis on the K_d values of NCp7 mutant proteins for SL3 RNA. The factor, F, by which the affinity for SL3 RNA changes for NCp7 mutants relative to that of the wild type was calculated from the tryptophan titration data in Table 1 and plotted on a Y-axis log scale. F = (K_d of mutant)/(K_d of WT). The standard deviations of F are listed in Table 1.

f1 knuckle and makes hydrophobic contacts with A319 in the SL3 tetraloop. It also stabilizes the protein structure through multiple hydrogen bonding and hydrophobic interactions. The observation that neither N5A nor N17A displayed a significant change in affinity for SL3 was unexpected. Either these two residues are not essential in NCp7−SL3 binding, or other interactions can compensate for the loss of H-bonds that should be caused by these mutations. This is in line with a previous report that virus replication and virion RNA content were largely retained upon mutation of N17.[72]

Single Mutants That Moderately Change Affinity. I24A, Q45A, M46A, and E21A show a moderately lower or higher affinity with K_d values ranging from 2 to 10 (or 0.5 to 0.1) times of that of WT, as does the double mutant, K14E/E21K.

Ile[24], Gln[45], and Met[46] are members of the hydrophobic core described above. These residues occupy positions on the same side of the two fingers, with Ile[24] and Gln[45] in equivalent positions. They all show steric interactions with the RNA molecule in the NMR structure.[1] The loss of affinity caused by these mutations indicates that these interactions contribute substantially to stabilization of the complex.

Another interesting single mutant in this group is E21A. Glu[21] is highly conserved and forms a salt bridge with Lys[14], which appears to stabilize the folding of the f1 knuckle.[1] Mutating Glu[21] to alanine destroys this salt bridge. One would expect such a change might result in a significant loss in the mutant protein's affinity for SL3 RNA. However, the affinity of E21A for SL3 RNA (K_d = 9 nM) turned out to be ~3 times higher than that of WT (29 nM). Although the mutation from Glu[21] to alanine destroys the salt bridge between Glu[21] and Lys[14], it also results in an increase of the protein's net charge from +9 to +10, which helps the protein to attract the negatively charged RNA.[43,50,73,74] Also, the f1 structure is stabilized by many other interactions, so the loss of the salt bridge may not be especially damaging. The bound RNA might also play a role in keeping f1 folded correctly.

Mutants That Significantly Change Affinity. F16A has a much larger K_d value than the WT (approximately 25-fold). [Similar changes are observed by both fluorescence and ITC (see Table 2).] This large reduction in the stability of the complex probably has a structural origin. As Phe[16] forms a hydrophobic cleft with several other amino acid residues to bind G318, this base may lose important contacts in the complex. It is also possible that substituting Phe[16] with Ala may lead to the collapse of the f1 knuckle, destabilizing both the protein and the complex. Comparison of $^{1}H-^{15}N$ HSQC spectra of SL3 bound to ^{15}N-labeled F16A and WT shows that there is little interaction between f1 residues and SL3 in F16A in contrast to the case in the WT, while f2 interacts strongly with SL3 in both F16A and the WT (L. Yang, W. Ouyang, D. Kerwood, and P. Borer, unpublished observations). These observations also agree with previously reported mutational studies.[24,46,72,75]

Salt Bridge Flipping Double Mutants. Two of the three double mutants, K33E/E42K and K38E/E51K, do not produce large changes in their affinity for SL3 RNA. However, the other double mutant, K14E/E21K, which contains mutations within the f1 knuckle, showed a moderately large change in the affinity for SL3. The K_d value of this double mutant for SL3 was calculated to be 140 nM. Compared to the other two double mutants, this observation indicated that structure of the f1 knuckle is more susceptible to mutations. The tryptophan titration curve of K14E/E21K does not fit well with the model described by eq 1 as shown in Figure 7. The interaction of this double mutant with SL3 RNA manifests as a biphasic binding isotherm. This anomalous behavior is echoed in the ITC data (Table 2 and Figure S3 of the Supporting Information), where

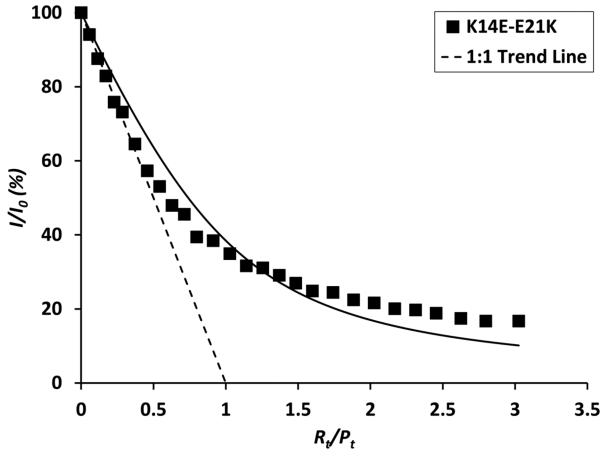

Figure 7. Tryptophan fluorescence titration curve of the K14E/E21K mutant with SL3 RNA. The fitted titration curve does not provide a good fit for the data points, indicating a different binding model might play a role in K14E/E21K's binding with SL3 RNA: (■) K21E/E21K and (---) a 1:1 complex with an infinite binding constant (K_d^{-1}).

curve fitting provides a low value for the average number of binding sites on the mutant protein (N = 0.79) and the lowest enthalpy of interaction ($\Delta H°$ = 6 kcal/mol) of all the mutants studied here.

The structure of the NCp7−SL3 complex may offer a clearer explanation of the differences in the affinity of the three salt bridge switching mutants for SL3. As shown in Figure 8, the

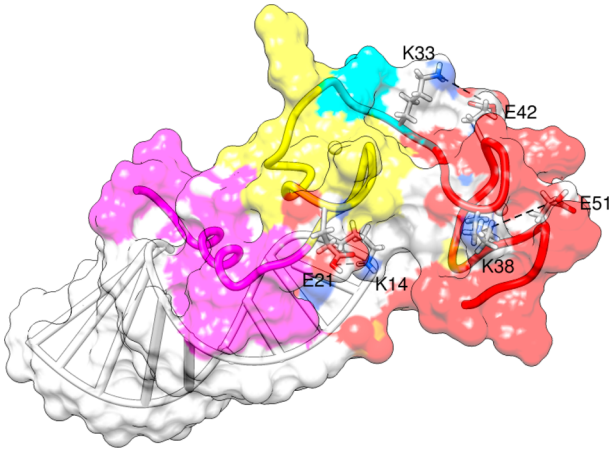

Figure 8. Positions of the three salt bridges in the NCp7−SL3 complex: white ribbon, SL3 RNA; colored ribbon, NCp7 protein; stick model, side chain atoms of Lys[14], Glu[21], Lys[33], Lys[38], Glu[42], and Glu[51]; magenta, N-terminal 3−10 helix of NCp7; yellow, N-terminal zinc finger (f1); cyan, linker region; red, C-terminal zinc finger (f2). The surface of the complex is shown in 50% transparency. Salt bridges are shown as dashed black lines between the two involved residues. Drawn from Protein Data Bank entry 1A1T using the UCSF Chimera package from the Resource for Biocomputing, Visualization, and Informatics at the University of California, San Francisco (supported by National Institutes of Health Grant P41 RR001081).[77]

Lys[33]−Glu[42] and Lys[38]−Glu[51] salt bridges are both directly exposed to solvent, while the Lys[14]−Glu[21] bridge is partially buried inside the complex, especially residue Lys[14]. Salt bridges exposed to the solvent may not contribute to stabilizing protein structures because of the interference of the solvent, but semiburied salt bridges like the Lys[14]−Glu[21] salt bridge can be a strong stabilizing force.[76] The moderate change of this double mutant's affinity indicates that even though the switched residues are still close to each other, their ability to form a salt bridge might be modified.

Comparison of Trp Titration and ITC Titration Results. The K_d values calculated from ITC titration data do not match exactly with those calculated from Trp titration data for the same mutant, but overall they show the same trends. The factor, F, which is the K_d ratio of a mutant to the WT, calculated from ITC data (see Table 2) shows that the results can be grouped in exactly the same way as discussed for the Trp titration results. The overall agreement between the two methods adds confidence to our interpretation of the relative contributions of the mutations reported here to the affinity of SL3 for NCp7.

Some of the differences in the K_d values calculated from the two methods may be attributed to the different nature of the assays. Tryptophan fluorescence quenching relies on the interaction of Trp[37] and the bases in bound RNA, while ITC experiments directly measure the heat released upon binding. The ITC experiment can be more accurate than tryptophan fluorescence titration, but this is true only at higher concentrations than are practical for NCp7−SL3 titrations. The ITC data, especially for the weakly bound complexes with F16A, I24A, and K14E/E21K, have poorly defined slopes at the ends of the titrations and may be noisy (see Figure 5 and Figure S3 of the Supporting Information). This causes more uncertainty in K_d, N, and $\Delta H°$. Tryptophan fluorescence titration has the advantage of being a convenient and straightforward assay with much higher sensitivity than ITC. The observation that ITC data follow the same trends as fluorescence titration data makes it unnecessary to perform ITC with each of the mutants.

The order of titration in the two assays is also different in this work. In fluorescence titrations, SL3 RNA is being titrated into NCp7 protein because it is more convenient to interpret the decrease in fluorescence than an increase. Our laboratory has published the conditions and a model to fit tryptophan fluorescence titrations in which NCp7 protein aliquots are added into a large excess of the SL3 RNA solution.[43] Excellent agreement in K_d values was found at the nearly physiological salt concentrations used in this work.

Conclusion. Most of the mutant NCp7 proteins did not exhibit a significant loss of affinity for SL3 RNA. This indicates that the side chain contacts of these mutated residues in wild-type NCp7 either contribute little to the stability of the complex or can be compensated by new contacts in the mutants. Strong conservation of many of these residues may arise from NC's interactions with other proteins or in other aspects of its many roles in HIV infection.

The F16A mutant exhibits a profound loss of affinity for SL3 RNA that is confirmed by both fluorescence titration and the ITC assay. This observation agrees with previously reported NMR structure and molecular dynamics analysis.[1,24] All of these indicate that Phe[16] is a key site in the NCp7−SL3 interaction that warrants further structural and functional study. Other interesting mutants that exhibit large changes in affinity include I24A and K14E/E21K; N5A and N17A may be of structural interest by virtue of their unchanged affinity even though key H-bonding and steric interactions are lost.

Tolerance to alanine mutagenesis in some highly conserved sites, such as Asn[5], Gly[19], Pro[31], and Gly[40], indicates that the key stabilizing interactions between NCp7 and SL3 might not be

dx.doi.org/10.1021/bi400125z | Biochemistry 2013, 52, 3358−3368

sensitive to the overall protein structure, yet the high degree of conservation of these residues suggests that they have important roles in other functions of NCp7, if not in the NCp7−SL3 interactions.

Tryptophan fluorescence titration and ITC are complementary methods, both of which have their own flaws and advantages. Both assays make reliable measurements of the K_d value. Both methods produce a mutually consistent picture of the RNA−protein interaction and confirm an $N = 1$ stoichiometry for NCp7−SL3 binding, which is shown in the complexes used in a previous NMR study.[1]

■ ASSOCIATED CONTENT

Supporting Information

Primer list for site-directed mutagenesis (Table S1), observed molecular masses for NCp7 mutants (Table S2), mutant list and amino acid sequences (Figure S1), sample fluorescence titration curves of NCp7 WT and mutants with SL3 (Figure S2), compilation of ITC curves of NCp7 WT and mutants with SL3 (Figure S3), and a summary of affinity changes by alanine mutations of different NCp7 residues (Figure S4). This material is available free of charge via the Internet at http://pubs.acs.org.

■ AUTHOR INFORMATION

Corresponding Author

*Department of Chemistry, Syracuse University, Syracuse, NY 13244-4100. E-mail: pnborer@syr.edu. Phone: (315) 443-2925.

Present Addresses

[§]W.O.: Department of Biochemistry, Albert Einstein College of Medicine, 1301 Morris Park Ave., Rm. 513, Price Center, Bronx, NY 10461.

[∥]S.O.: Regeneron Pharmaceuticals Inc., 777 Old Saw Mill River Rd., Tarrytown, NY 10591.

[⊥]M.P.M.: AptaMatrix, Inc., 100 Intrepid Ln., Suite 1, Syracuse, NY 13205.

[@]Y.L.: 19 Baker St., Apt. 1, Belmont, MA 02478.

Funding

Supported in part by National Institutes of Health Grant R01 GM32691.

Notes

The authors declare no competing financial interest.

■ ACKNOWLEDGMENTS

We thank Dana Schaefer and James Crill, II, for general assistance in the lab. We thank Drs. Christopher DeCiantis and Richard Yule for advice and help with SL3−NCp7 titration. We thank Dr. Deborah Kerwood for assistance with mass spectrometry experiments. We thank David Kiemle and the ATS facility at SUNY College of Environmental Science and Forestry for access to the mass spectrometry instrument. We thank Drs. Michael Cosgrove and Anamika Patel in the Department of Biology at Syracuse University for assistance with the AUC experiment. We thank Dr. Stephan Wilkens and Rebecca Oot at SUNY Upstate Medical University for access and assistance to the ITC instrument.

■ ABBREVIATIONS

NCp7, 55-amino acid nucleocapsid protein of HIV-1 (human immunodeficiency virus); SL3, short stem−loop segment of RNA from the 5′-leader region of HIV-1; NC, nucleocapsid; FPLC, fast protein liquid chromatography; SDS−PAGE, sodium dodecyl sulfate−polyacrylamide gel electrophoresis; ITC, isothermal titration calorimetry; AUC, analytical ultracentrifugation; MALDI-TOF, matrix-assisted laser desorption ionization time-of-flight; IPTG, isopropyl β-D-1-thiogalactopyranoside; TCEP·HCl, tris(2-carboxyethyl)phosphine hydrochloride; PMSF, phenylmethanesulfonyl fluoride; PEI, polyethyleneimine; avg, average; SD, standard deviation; TFA, trifluoroacetic acid; K_d, dissociation constant.

■ REFERENCES

(1) De Guzman, R. N., Wu, Z. R., Stalling, C. C., Pappalardo, L., Borer, P. N., and Summers, M. F. (1998) Structure of the HIV-1 nucleocapsid protein bound to the SL3 ψ-RNA recognition element. *Science 279*, 384−388.

(2) Henderson, L. E., Bowers, M. A., Sowder, R. C., II, Serabyn, S. A., Johnson, D. G., Bess, J. W., Jr., Arthur, L. O., Bryant, D. K., and Fenselau, C. (1992) Gag proteins of the highly replicative MN strain of human immunodeficiency virus type 1: Posttranslational modifications, proteolytic processings, and complete amino acid sequences. *J. Virol. 66*, 1856−1865.

(3) Lapadat-Tapolsky, M., Gabus, C., Rau, M., and Darlix, J. L. (1997) Possible roles of HIV-1 nucleocapsid protein in the specificity of proviral DNA synthesis and in its variability. *J. Mol. Biol. 268*, 250−260.

(4) Briggs, J. A., Johnson, M. C., Simon, M. N., Fuller, S. D., and Vogt, V. M. (2006) Cryo-electron microscopy reveals conserved and divergent features of gag packing in immature particles of Rous sarcoma virus and human immunodeficiency virus. *J. Mol. Biol. 355*, 157−168.

(5) Krishnamoorthy, G., Roques, B., Darlix, J. L., and Mely, Y. (2003) DNA condensation by the nucleocapsid protein of HIV-1: A mechanism ensuring DNA protection. *Nucleic Acids Res. 31*, 5425−5432.

(6) Buckman, J. S., Bosche, W. J., and Gorelick, R. J. (2003) Human immunodeficiency virus type 1 nucleocapsid Zn^{2+} fingers are required for efficient reverse transcription, initial integration processes, and protection of newly synthesized viral DNA. *J. Virol. 77*, 1469−1480.

(7) Linial, M. L., and Miller, A. D. (1990) Retroviral RNA packaging: Sequence requirements and implications. *Curr. Top. Microbiol. Immunol. 157*, 125−152.

(8) Gelderblom, H. R. (1991) Assembly and morphology of HIV: Potential effect of structure on viral function. *AIDS 5*, 617−637.

(9) Coffin, J. M., Hughes, S. H., and Varmus, H. (1997) *Retroviruses*, Cold Spring Harbor Laboratory Press, Plainview, NY.

(10) Gallo, R. C., and Jay, G., Eds. (1991) *The Human Retroviruses*, Academic Press, New York.

(11) Levin, J. G., Mitra, M., Mascarenhas, A., and Musier-Forsyth, K. (2010) Role of HIV-1 nucleocapsid protein in HIV-1 reverse transcription. *RNA Biol. 7*, 754−774.

(12) Prats, A. C., Sarih, L., Gabus, C., Litvak, S., Keith, G., and Darlix, J. L. (1988) Small finger protein of avian and murine retroviruses has nucleic acid annealing activity and positions the replication primer tRNA onto genomic RNA. *EMBO J. 7*, 1777−1783.

(13) Druillennec, S., Caneparo, A., de Rocquigny, H., and Roques, B. P. (1999) Evidence of interactions between the nucleocapsid protein NCp7 and the reverse transcriptase of HIV-1. *J. Biol. Chem. 274*, 11283−11288.

(14) Lener, D., Tanchou, V., Roques, B. P., Le Grice, S. F., and Darlix, J. L. (1998) Involvement of HIV-I nucleocapsid protein in the recruitment of reverse transcriptase into nucleoprotein complexes formed in vitro. *J. Biol. Chem. 273*, 33781−33786.

(15) de Rocquigny, H., Caneparo, A., Delaunay, T., Bischerour, J., Mouscadet, J. F., and Roques, B. P. (2000) Interactions of the C-terminus of viral protein R with nucleic acids are modulated by its N-terminus. *Eur. J. Biochem. 267*, 3654−3660.

(16) Grohmann, D., Godet, J., Mely, Y., Darlix, J. L., and Restle, T. (2008) HIV-1 nucleocapsid traps reverse transcriptase on nucleic acid substrates. *Biochemistry 47*, 12230−12240.

(17) Bampi, C., Jacquenet, S., Lener, D., Decimo, D., and Darlix, J. L. (2004) The chaperoning and assistance roles of the HIV-1 nucleocapsid protein in proviral DNA synthesis and maintenance. *Int. J. Biochem. Cell Biol. 36*, 1668−1686.
(18) Williams, M. C., Rouzina, I., Wenner, J. R., Gorelick, R. J., Musier-Forsyth, K., and Bloomfield, V. A. (2001) Mechanism for nucleic acid chaperone activity of HIV-1 nucleocapsid protein revealed by single molecule stretching. *Proc. Natl. Acad. Sci. U.S.A. 98*, 6121−6126.
(19) Fu, W., Gorelick, R. J., and Rein, A. (1994) Characterization of human immunodeficiency virus type 1 dimeric RNA from wild-type and protease-defective virions. *J. Virol. 68*, 5013−5018.
(20) Jalalirad, M., and Laughrea, M. (2010) Formation of immature and mature genomic RNA dimers in wild-type and protease-inactive HIV-1: Differential roles of the Gag polyprotein, nucleocapsid proteins NCp15, NCp9, NCp7, and the dimerization initiation site. *Virology 407*, 225−236.
(21) Wills, J. W., and Craven, R. C. (1991) Form, function, and use of retroviral gag proteins. *AIDS 5*, 639−654.
(22) Oertle, S., and Spahr, P. F. (1990) Role of the gag polyprotein precursor in packaging and maturation of Rous sarcoma virus genomic RNA. *J. Virol. 64*, 5757−5763.
(23) Damgaard, C. K., Dyhr-Mikkelsen, H., and Kjems, J. (1998) Mapping the RNA binding sites for human immunodeficiency virus type-1 gag and NC proteins within the complete HIV-1 and -2 untranslated leader regions. *Nucleic Acids Res. 26*, 3667−3676.
(24) Mori, M., Dietrich, U., Manetti, F., and Botta, M. (2010) Molecular dynamics and DFT study on HIV-1 nucleocapsid protein-7 in complex with viral genome. *J. Chem. Inf. Model. 50*, 638−650.
(25) Mori, M., Schult-Dietrich, P., Szafarowicz, B., Humbert, N., Debaene, F., Sanglier-Cianferani, S., Dietrich, U., Mely, Y., and Botta, M. (2012) Use of virtual screening for discovering antiretroviral compounds interacting with the HIV-1 nucleocapsid protein. *Virus Res. 169*, 377−387.
(26) Shubsda, M. F., Paoletti, A. C., Hudson, B. S., and Borer, P. N. (2002) Affinities of packaging domain loops in HIV-1 RNA for the nucleocapsid protein. *Biochemistry 41*, 5276−5282.
(27) Clever, J., Sassetti, C., and Parslow, T. G. (1995) RNA secondary structure and binding sites for gag gene products in the 5′ packaging signal of human immunodeficiency virus type 1. *J. Virol. 69*, 2101−2109.
(28) Clever, J. L., Eckstein, D. A., and Parslow, T. G. (1999) Genetic dissociation of the encapsidation and reverse transcription functions in the 5′ R region of human immunodeficiency virus type 1. *J. Virol. 73*, 101−109.
(29) Clever, J. L., and Parslow, T. G. (1997) Mutant human immunodeficiency virus type 1 genomes with defects in RNA dimerization or encapsidation. *J. Virol. 71*, 3407−3414.
(30) McBride, M. S., and Panganiban, A. T. (1996) The human immunodeficiency virus type 1 encapsidation site is a multipartite RNA element composed of functional hairpin structures. *J. Virol. 70*, 2963−2973.
(31) McBride, M. S., Schwartz, M. D., and Panganiban, A. T. (1997) Efficient encapsidation of human immunodeficiency virus type 1 vectors and further characterization of cis elements required for encapsidation. *J. Virol. 71*, 4544−4554.
(32) Hayashi, T., Shioda, T., Iwakura, Y., and Shibuta, H. (1992) RNA packaging signal of human immunodeficiency virus type 1. *Virology 188*, 590−599.
(33) Hayashi, T., Ueno, Y., and Okamoto, T. (1993) Elucidation of a conserved RNA stem-loop structure in the packaging signal of human immunodeficiency virus type 1. *FEBS Lett. 327*, 213−218.
(34) South, T. L., and Summers, M. F. (1993) Zinc- and sequence-dependent binding to nucleic acids by the N-terminal zinc finger of the HIV-1 nucleocapsid protein: NMR structure of the complex with the *ψ*-site analog, dACGCC. *Protein Sci. 2*, 3−19.
(35) Summers, M. F., Henderson, L. E., Chance, M. R., Bess, J. W., Jr., South, T. L., Blake, P. R., Sagi, I., Perez-Alvarado, G., Sowder, R. C., III, Hare, D. R., et al. (1992) Nucleocapsid zinc fingers detected in retroviruses: EXAFS studies of intact viruses and the solution-state structure of the nucleocapsid protein from HIV-1. *Protein Sci. 1*, 563−574.
(36) Delahunty, M. D., South, T. L., Summers, M. F., and Karpel, R. L. (1992) Nucleic acid interactive properties of a peptide corresponding to the N-terminal zinc finger domain of HIV-1 nucleocapsid protein. *Biochemistry 31*, 6461−6469.
(37) Ramboarina, S., Druillennec, S., Morellet, N., Bouaziz, S., and Roques, B. P. (2004) Target specificity of human immunodeficiency virus type 1 NCp7 requires an intact conformation of its CCHC N-terminal zinc finger. *J. Virol. 78*, 6682−6687.
(38) Mark-Danieli, M., Laham, N., Kenan-Eichler, M., Castiel, A., Melamed, D., Landau, M., Bouvier, N. M., Evans, M. J., and Bacharach, E. (2005) Single point mutations in the zinc finger motifs of the human immunodeficiency virus type 1 nucleocapsid alter RNA binding specificities of the gag protein and enhance packaging and infectivity. *J. Virol. 79*, 7756−7767.
(39) Aldovini, A., and Young, R. A. (1990) Mutations of RNA and protein sequences involved in human immunodeficiency virus type 1 packaging result in production of noninfectious virus. *J. Virol. 64*, 1920−1926.
(40) Gorelick, R. J., Henderson, L. E., Hanser, J. P., and Rein, A. (1988) Point mutants of Moloney murine leukemia virus that fail to package viral RNA: Evidence for specific RNA recognition by a "zinc finger-like" protein sequence. *Proc. Natl. Acad. Sci. U.S.A. 85*, 8420−8424.
(41) Dupraz, P., Oertle, S., Meric, C., Damay, P., and Spahr, P. F. (1990) Point mutations in the proximal Cys-His box of Rous sarcoma virus nucleocapsid protein. *J. Virol. 64*, 4978−4987.
(42) Grigorov, B., Decimo, D., Smagulova, F., Pechoux, C., Mougel, M., Muriaux, D., and Darlix, J. L. (2007) Intracellular HIV-1 Gag localization is impaired by mutations in the nucleocapsid zinc fingers. *Retrovirology 4*, 54.
(43) Athavale, S. S., Ouyang, W., McPike, M. P., Hudson, B. S., and Borer, P. N. (2010) Effects of the nature and concentration of salt on the interaction of the HIV-1 nucleocapsid protein with SL3 RNA. *Biochemistry 49*, 3525−3533.
(44) Zhang, Z., Xi, X., Scholes, C. P., and Karim, C. B. (2008) Rotational dynamics of HIV-1 nucleocapsid protein NCp7 as probed by a spin label attached by peptide synthesis. *Biopolymers 89*, 1125−1135.
(45) Xi, X., Sun, Y., Karim, C. B., Grigoryants, V. M., and Scholes, C. P. (2008) HIV-1 nucleocapsid protein NCp7 and its RNA stem loop 3 partner: Rotational dynamics of spin-labeled RNA stem loop 3. *Biochemistry 47*, 10099−10110.
(46) Fisher, R. J., Fivash, M. J., Stephen, A. G., Hagan, N. A., Shenoy, S. R., Medaglia, M. V., Smith, L. R., Worthy, K. M., Simpson, J. T., Shoemaker, R., McNitt, K. L., Johnson, D. G., Hixson, C. V., Gorelick, R. J., Fabris, D., Henderson, L. E., and Rein, A. (2006) Complex interactions of HIV-1 nucleocapsid protein with oligonucleotides. *Nucleic Acids Res. 34*, 472−484.
(47) Morellet, N., de Rocquigny, H., Mely, Y., Jullian, N., Demene, H., Ottmann, M., Gerard, D., Darlix, J. L., Fournie-Zaluski, M. C., and Roques, B. P. (1994) Conformational behaviour of the active and inactive forms of the nucleocapsid NCp7 of HIV-1 studied by 1H NMR. *J. Mol. Biol. 235*, 287−301.
(48) Ottmann, M., Gabus, C., and Darlix, J. L. (1995) The central globular domain of the nucleocapsid protein of human immunodeficiency virus type 1 is critical for virion structure and infectivity. *J. Virol. 69*, 1778−1784.
(49) Cimarelli, A., Sandin, S., Hoglund, S., and Luban, J. (2000) Basic residues in human immunodeficiency virus type 1 nucleocapsid promote virion assembly via interaction with RNA. *J. Virol. 74*, 3046−3057.
(50) Schmalzbauer, E., Strack, B., Dannull, J., Guehmann, S., and Moelling, K. (1996) Mutations of basic amino acids of NCp7 of human immunodeficiency virus type 1 affect RNA binding in vitro. *J. Virol. 70*, 771−777.

(51) Poon, D. T., Wu, J., and Aldovini, A. (1996) Charged amino acid residues of human immunodeficiency virus type 1 nucleocapsid p7 protein involved in RNA packaging and infectivity. *J. Virol. 70*, 6607−6616.
(52) Darlix, J. L., Cristofari, G., Rau, M., Pechoux, C., Berthoux, L., and Roques, B. (2000) Nucleocapsid protein of human immunodeficiency virus as a model protein with chaperoning functions and as a target for antiviral drugs. *Adv. Pharmacol. 48*, 345−372.
(53) Berthoux, L., Pechoux, C., and Darlix, J. L. (1999) Multiple effects of an anti-human immunodeficiency virus nucleocapsid inhibitor on virus morphology and replication. *J. Virol. 73*, 10000−10009.
(54) de Rocquigny, H., Shvadchak, V., Avilov, S., Dong, C. Z., Dietrich, U., Darlix, J. L., and Mely, Y. (2008) Targeting the viral nucleocapsid protein in anti-HIV-1 therapy. *Mini-Rev. Med. Chem. 8*, 24−35.
(55) Goldschmidt, V., Miller Jenkins, L. M., de Rocquigny, H., Darlix, J.-L., and Mély, Y. (2010) The nucleocapsid protein of HIV-1 as a promising therapeutic target for antiviral drugs. *HIV Ther. 4*, 179−198.
(56) Miller Jenkins, L. M., Ott, D. E., Hayashi, R., Coren, L. V., Wang, D., Xu, Q., Schito, M. L., Inman, J. K., Appella, D. H., and Appella, E. (2010) Small-molecule inactivation of HIV-1 NCp7 by repetitive intracellular acyl transfer. *Nat. Chem. Biol. 6*, 887−889.
(57) Cruceanu, M., Stephen, A. G., Beuning, P. J., Gorelick, R. J., Fisher, R. J., and Williams, M. C. (2006) Single DNA molecule stretching measures the activity of chemicals that target the HIV-1 nucleocapsid protein. *Anal. Biochem. 358*, 159−170.
(58) Stephen, A. G., Rein, A., Fisher, R. J., and Shoemaker, R. H. (2003) The nucleocapsid protein as a target for novel anti-HIV drugs. *Current Drug Discovery*, 33−36.
(59) Stephen, A. G., Worthy, K. M., Towler, E., Mikovits, J. A., Sei, S., Roberts, P., Yang, Q. E., Akee, R. K., Klausmeyer, P., McCloud, T. G., Henderson, L., Rein, A., Covell, D. G., Currens, M., Shoemaker, R. H., and Fisher, R. J. (2002) Identification of HIV-1 nucleocapsid protein: Nucleic acid antagonists with cellular anti-HIV activity. *Biochem. Biophys. Res. Commun. 296*, 1228−1237.
(60) Sartori, D. A., Miller, B., Biebach, U., and Farrell, N. (2000) Modulation of the chemical and biological properties of trans platinum complexes: Monofunctional platinum complexes containing one nucleobase as potential antiviral chemotypes. *JBIC, J. Biol. Inorg. Chem. 5*, 575−583.
(61) Quintal, S., Viegas, A., Erhardt, S., Cabrita, E. J., and Farrell, N. P. (2012) Platinated DNA affects zinc finger conformation. Interaction of a platinated single-stranded oligonucleotide and the C-terminal zinc finger of nucleocapsid protein HIVNCp7. *Biochemistry 51*, 1752−1761.
(62) Lin, Y. (2002) Database and algorithmic applications in nucleic acid sequence, structure and NMR frequencies, and an efficient chemical depiction. Ph.D. Dissertation, pp 1−218, Syracuse University, Syracuse, NY.
(63) Paoletti, A. C., Shubsda, M. F., Hudson, B. S., and Borer, P. N. (2002) Affinities of the nucleocapsid protein for variants of SL3 RNA in HIV-1. *Biochemistry 41*, 15423−15428.
(64) Cornille, F., Mely, Y., Ficheux, D., Savignol, I., Gerard, D., Darlix, J. L., Fournie-Zaluski, M. C., and Roques, B. P. (1990) Solid phase synthesis of the retroviral nucleocapsid protein NCp10 of Moloney murine leukaemia virus and related "zinc-fingers" in free SH forms. Influence of zinc chelation on structural and biochemical properties. *Int. J. Pept. Protein Res. 36*, 551−558.
(65) Vuilleumier, C., Bombarda, E., Morellet, N., Gerard, D., Roques, B. P., and Mely, Y. (1999) Nucleic acid sequence discrimination by the HIV-1 nucleocapsid protein NCp7: A fluorescence study. *Biochemistry 38*, 16816−16825.
(66) Bourbigot, S., Ramalanjaona, N., Boudier, C., Salgado, G. F., Roques, B. P., Mely, Y., Bouaziz, S., and Morellet, N. (2008) How the HIV-1 nucleocapsid protein binds and destabilises the (−)primer binding site during reverse transcription. *J. Mol. Biol. 383*, 1112−1128.
(67) Lee, B. M., De Guzman, R. N., Turner, B. G., Tjandra, N., and Summers, M. F. (1998) Dynamical behavior of the HIV-1 nucleocapsid protein. *J. Mol. Biol. 279*, 633−649.
(68) Studier, F. W., Rosenberg, A. H., Dunn, J. J., and Dubendorff, J. W. (1990) Use of T7 RNA polymerase to direct expression of cloned genes. *Methods Enzymol. 185*, 60−89.
(69) Schuck, P. (2000) Size-distribution analysis of macromolecules by sedimentation velocity ultracentrifugation and Lamm equation modeling. *Biophys. J. 78*, 1606−1619.
(70) Ouyang, W. (2011) Mutational Analysis of HIV-1 Nucleocapsid Protein and Methods Development for Aptamer Discovery. Ph.D. Dissertation, pp 1−302, Syracuse University, Syracuse, NY.
(71) Salim, N. N., and Feig, A. L. (2009) Isothermal titration calorimetry of RNA. *Methods 47*, 198−205.
(72) Dorfman, T., Luban, J., Goff, S. P., Haseltine, W. A., and Gottlinger, H. G. (1993) Mapping of functionally important residues of a cysteine-histidine box in the human immunodeficiency virus type 1 nucleocapsid protein. *J. Virol. 67*, 6159−6169.
(73) Prats, A. C., Housset, V., de Billy, G., Cornille, F., Prats, H., Roques, B., and Darlix, J. L. (1991) Viral RNA annealing activities of the nucleocapsid protein of Moloney murine leukemia virus are zinc independent. *Nucleic Acids Res. 19*, 3533−3541.
(74) Surovoy, A., Dannull, J., Moelling, K., and Jung, G. (1993) Conformational and nucleic acid binding studies on the synthetic nucleocapsid protein of HIV-1. *J. Mol. Biol. 229*, 94−104.
(75) Wu, H., Mitra, M., McCauley, M. J., Thomas, J. A., Rouzina, I., Musier-Forsyth, K., Williams, M. C., and Gorelick, R. J. (2013) Aromatic residue mutations reveal direct correlation between HIV-1 nucleocapsid protein's nucleic acid chaperone activity and retroviral replication. *Virus Res. 171*, 263−277.
(76) Dong, F., and Zhou, H. X. (2002) Electrostatic contributions to T4 lysozyme stability: Solvent-exposed charges versus semi-buried salt bridges. *Biophys. J. 83*, 1341−1347.
(77) Pettersen, E. F., Goddard, T. D., Huang, C. C., Couch, G. S., Greenblatt, D. M., Meng, E. C., and Ferrin, T. E. (2004) UCSF Chimera: A visualization system for exploratory research and analysis. *J. Comput. Chem. 25*, 1605−1612.